HHS Public Access

Author manuscript

J Am Chem Soc. Author manuscript; available in PMC 2019 October 17.

Published in final edited form as:

J Am Chem Soc. 2018 October 17; 140(41): 13205–13208. doi:10.1021/jacs.8b08659.

Sacrificial Cobalt−Carbon Bond Homolysis in Coenzyme B_{12} as a Cofactor Conservation Strategy

Gregory C. Campanello[†], **Markus Ruetz**[†], **Greg J. Dodge**[†,‡], **Harsha Gouda**[†,§], **Aditi Gupta**[†], **Umar T. Twahir**[||], **Michelle M. Killian**[⊥], **David Watkins**[#], **David S. Rosenblatt**[#], **Thomas C. Brunold**[⊥], **Kurt Warncke**[||], **Janet L. Smith**[†,‡], **Ruma Banerjee**[*,†]

[†]Department of Biological Chemistry, University of Michigan, Ann Arbor, Michigan 48109-0600, United States

[‡]Life Sciences Institute, University of Michigan, Ann Arbor, Michigan 48109-0600, United States

[§]Indian Institute of Science Education and Research, Pune 411008, India

[||]Department of Physics, Emory University, Atlanta, Georgia 30322-2430, United States

[⊥]Department of Chemistry, University of Wisconsin−Madison, Madison, Wisconsin 53706, United States

[#]Department of Human Genetics, McGill University, Montreal, Quebec H3A 1B1, Canada

Abstract

A sophisticated intracellular trafficking pathway in humans is used to tailor vitamin B_{12} into its active cofactor forms, and to deliver it to two known B_{12}-dependent enzymes. Herein, we report an unexpected strategy for cellular retention of B_{12}, an essential and reactive cofactor. If methylmalonyl-CoA mutase is unavailable to accept the coenzyme B_{12} product of adenosyltransferase, the latter catalyzes homolytic scission of the cobalt−carbon bond in an unconventional reversal of the nucleophilic displacement reaction that was used to make it. The resulting homolysis product binds more tightly to adenosyltransferase than does coenzyme B_{12}, facilitating cofactor retention. We have trapped, and characterized spectroscopically, an intermediate in which the cobalt−carbon bond is weakened prior to being broken. The physiological relevance of this sacrificial catalytic activity for cofactor retention is supported by the significantly lower coenzyme B_{12} concentration in patients with dysfunctional methylmalonyl-CoA mutase but normal adenosyltransferase activity.

The landmark accomplishment of elucidating the structure of vitamin B_{12}[1] was followed by clinical genetics studies on patients with inborn errors of B_{12} metabolism, which hinted at a complex pathway for its intracellular trafficking.[2] These studies revealed that at least seven protein handlers assimilate and escort this reactive cofactor[3] to the two enzymes that use it:

[*]Corresponding Author: rbanerje@umich.edu.

The Supporting Information is available free of charge on the ACS Publications website at DOI: 10.1021/jacs.8b08659.
Materials and methods (PDF)

The authors declare no competing financial interest.
Coordinates for the ATR structures have been deposited in the PDB (6D5X, 6D5K)

methylmalonyl-CoA mutase (MCM)[4] and methionine synthase (MS).[5] MCM, a mitochondrial enzyme, uses 5′-deoxyadenosylcobalamin (AdoCbl or coenzyme B_{12}) and isomerizes (*R*)-methylmalonyl-CoA to succinyl-CoA. AdoCbl is synthesized by adenosyltransferase (ATR), which catalyzes the adenosylation of cob(I)alamin by ATP in a direct nucleophilic displacement reaction that leads to cobalt−carbon (Co−C) bond formation yielding AdoCbl and inorganic triphosphate (PPP_i)[6] (Figure 1a). ATR also delivers the AdoCbl product directly to MCM, thereby averting cofactor loss by release into solution.[6] Herein, we report the unusual chemical versatility of ATR, which catalyzes homolytic cleavage of the newly formed Co−C bond of AdoCbl in the presence of PPP_i if MCM is unavailable as an acceptor. Unlike AdoCbl, the resulting cob(II)alamin product is tightly bound to human ATR, reducing loss of the rare but essential cofactor into solution. Patients with mutations in MCM but with normal ATR exhibit significantly reduced AdoCbl levels, supporting the relevance of this cofactor sequestration mechanism in a cellular milieu.

ATR is a homotrimer that binds AdoCbl in a five-coordinate (5C) “base-off” state[7] in which the lower axial ligand, dimethylbenzimidazole (DMB), is displaced from cobalt. In contrast, MCM, which also binds AdoCbl in a base-off state, fills the lower axial position with a histidine residue.[8] The change from 5- to 6C AdoCbl is accompanied by large spectral changes, which allow facile monitoring of the cofactor’s movement between the active sites. Complete cofactor transfer from ATR·AdoCbl to MCM is observed upon mixing the two proteins as indicated by a shift in the absorption maximum from 455 to 530 nm (Figure 1b). Transfer of AdoCbl from ATR (K_d = 0.96 ± 0.31 μM) to MCM (K_d = 0.27 ± 0.11 μM) is thermodynamically favored (Table S1). The reverse transfer was not observed even in the presence of excess ATR (Figure S1), which contrasts with the bidirectional transfer of AdoCbl observed with the homologous *Methylobacterium extorquens* proteins.[6]

The fate of the newly synthesized and precious AdoCbl product was examined in the absence of MCM. Addition of PPP_i to human ATR·AdoCbl to mimic the initially formed ternary product complex, elicited an unexpected spectral change (Figure 1c) forming intermediate “X” with absorption maxima at 388 and 439 nm. Whereas X was stable under anaerobic conditions, it converted under aerobic conditions to a new species with a 465 nm absorption maximum (Figure 1d), which is spectroscopically identical to 4C cob(II)alamin bound to ATR·ATP (Figure S2). We hypothesized that PPP_i binding to ATR·AdoCbl weakened the Co−C bond forming X, which then underwent homolytic bond cleavage yielding cob(II)-alamin and Ado (Figure 1e). Whereas geminate recombination of the radical pair predominated under anaerobic conditions, irreversible interception of Ado by O_2 shifted the equilibrium away from X to cob(II)alamin.

To test this hypothesis, we characterized the products obtained upon addition of PPP_i to ATR·AdoCbl. The spectrum of X is very similar to that of base-off neopentylcobalamin (NpCbl) (Figure 1c, inset). Steric strain from the bulky neopentyl group weakens the Co−C bond and leads to a 10^6-fold enhancement of the homolysis rate with NpCbl compared to AdoCbl.[9,10] Although the precise nature of X is unclear, the spectral similarity between it and NpCbl suggests stabilization of an intermediate in which the Co−C bond is weakened prior to being homolytically cleaved. Evidence that X is diamagnetic and that 4C

cob(II)alamin is formed under aerobic conditions was obtained by EPR spectroscopy. The large g spread and substantial Co hyperfine splittings are diagnostic of a square planar Co(II) coordination environment (Figures 2a and S3). Consistent with these results, the corresponding MCD spectrum showed an intense positively signed feature at 12 500 cm^{-1} that is characteristic of 4C cob(II)alamin. This feature is considerably red-shifted from its counterpart in cob(II)inamide, which has an axial water ligand in solution (Figure 2b and S4).[11] The fate of Ado· was investigated by NMR spectroscopy using [U−^{13}C-Ado]-Cbl. The ^{1}H and ^{13}C chemical shifts of the product (Figure S5 and Tables S2 and S3) were nearly identical to those reported previously for 5′-hydroperoxyadenosine formed during aerobic photolysis of AdoCbl.[12] However, while 5′-hydroperoxyadenosine arises in aqueous solution from hydrolysis of a 5′-peroxy-AdoCbl intermediate and yields cob(III)alamin, 4C cob(II)alamin is produced in the ATR active site. Hence, 5′-hydroperoxyadenosine formed in the ATR reaction likely results from quenching of the initially formed alkylperoxy (Ado-OO·) radical. The source of the hydrogen atom is not known.

We solved the structure of human ATR·ATP crystals soaked with AdoCbl (Table S4). Electron density for AdoCbl was observed in two active sites (with occupancies of 1.00 and 0.86) and for ATP in the third site (Figures 2c and S6). The adenosine moieties in the sites containing ATP[13] and AdoCbl are virtually superimposable (Figure 2d), held via electrostatic and hydrophobic interactions. Fortuitously, we also obtained a structure with AdoCbl and PPP_i bound (Figure 2e), which we ascribe to contaminating PPP_i in the ATP sample and to its high affinity for ATR·AdoCbl (Table S1). The structures in the absence and presence of ATP are very similar, and at the current resolution, do not provide insights into how PPP_i labilizes the Co−C bond. AdoCbl is bound in a base-off state with Phe170 on a hydrophobic loop wedging between the DMB and the corrin ring, precluding water coordination (Figure 2f). The DMB tail in this structure is fully resolved in contrast to the *Lactobacillus reuteri* ATR structure where it is disordered.[14] While AdoCbl transfer to MCM (k = 0.63 ± 0.06 min^{-1}) and sacrificial formation of 5′-hydroperoxyadenosine and cob(II)alamin (k = 0.082 ± 0.01 min^{-1}) both proceed slowly, the former is favored ~8-fold over the latter. We note that CblC, a B_{12} chaperone with decyanase and dealkylase activities, also exhibits low reaction rates (~0.003−0.2 min^{-1}) that nevertheless support cellular B processing.[15,16] Apparently, the low reaction rates are sufficient to support low flux through the B_{12} trafficking pathway in which fidelity is prioritized over speed.[17]

What could be the physiological significance of AdoCbl synthesis by ATR at the expense of three ATP equivalents only to be followed by its cleavage in the absence of MCM? The kinetic choices facing the newly formed ternary ATR·AdoCbl·PPP_i complex in the absence of AdoCbl transfer to MCM are to form cob(II)alamin, as a strategy to sequester the cofactor or to release AdoCbl into solution. From a thermodynamic standpoint, binding of ATP and cob(II)alamin (K_d = 0.08 ± 0.01 μM) to ATR is favored over AdoCbl (K_d = 0.96 ± 0.31 μM) (Table S1). Our model predicts that AdoCbl levels should be reduced in MCM deficiency even though AdoCbl synthesis by ATR is unimpaired. To test this model, we examined AdoCbl levels in normal versus patient fibroblasts. In control fibroblasts (n = 192), 15.1 ± 3.4% of the intracellular B_{12} pool is AdoCbl (Figure 3a); the majority exists as methylcobalamin. As expected for fibroblasts with ATR deficiency (due to mutations in the *cblB* locus), the AdoCbl pool size is reduced (3.0 ± 2.1%, n = 45, p < 0.0005). Consistent

with our model, the AdoCbl pool is smaller in patients with MCM (*mut*) deficiency, which is differentiated into groups containing either low (8.3 ± 6.9% in mut^{-}, $n = 53$, $p < 0.0005$) or undetectable (8.1 ± 4.4% in mut^{0}, $n = 195$, $p < 0.0005$) mutase activity.

Because of its low intracellular concentration, it is unlikely that free PPP_i binds to the binary ATR·AdoCbl complex (K_d =0.42 ± 0.08 μM, Figure S7) to trigger Co−C bond homolysis. Instead, we predict that the fate of AdoCbl is dictated by the kinetics of its transfer to MCM from the newly formed product complex versus Co−C bond homolysis. This model is indirectly supported by the properties of the R186Q patient mutation.[18] The in vitro activity of R186Q (11 ± 3.6 min^{-1}) and wild-type (14.8 ± 3.5 min^{-1}) ATR are comparable. Arg186 forms an intersubunit salt bridge with Asp90 only when B_{12} is bound (Figure 2d). The mutant protein binds B_{12} in the base-on state as monitored by EPR and absorption spectroscopy (Figure 3b,c), revealing the tenuous hold of ATR on the base-off state. The homologous mutation in *L. reuteri* ATR also led to bound base-on B_{12}.[19] The R186Q mutation destabilizes the ternary ATR·AdoCbl·PPP_i complex but does not affect ATP binding (Figure S8 and Tables S1 and S5). Furthermore, while the affinity for cob(II)alamin is unaffected (≤0.2 μM), the affinity for AdoCbl is significantly diminished. The product of Co−C bond homolysis in the R186Q mutant resembles base-on 6C Np-Cbl (Figure 2c, inset) but is only seen when ATR active sites are present in vast excess over AdoCbl. Hence, the inability to sequester AdoCbl via direct transfer to MCM predisposes the R186Q mutant to cofactor release into solution (Figure 3d). We speculate that the twin challenges of reducing base-on cob(II)alamin (which has a lower redox potential than the base-off form[20]), and weakened affinity for AdoCbl, contribute to methylmalonic aciduria in patients with the biallelic R186Q mutation. We recently reported that itaconyl-CoA inactivates MCM by rapid cob(II)alamin accumulation on the enzyme.[21] Human MCM binds cob(II)alamin with a lower affinity than AdoCbl (Table S1), which begs the question as to how cob(II)alamin loss is averted from MCM into solution.

A cytoplasmic strategy for cofactor sequestration is exemplified by MS, whose synthesis is translationally up-regulated by B_{12}.[22] Prioritization of the B_{12} supply for MS, an essential enzyme, over MCM, which serves an anaplerotic function, is suggested by the prevalence of holo-MS (~100%)[23] versus fractional B_{12} saturation of MCM (~25%)[24] in liver. Furthermore, under conditions of B_{12} deficiency, the magnitude of cofactor loss from MCM is greater than from MS.[24] We now report a cellular strategy for B_{12} retention that exploits an unprecedented chemical versatility whereby AdoCbl is synthesized via nucleophilic chemistry but cleaved via radical chemistry within the same active site. The mechanism for mitochondrial import of B_{12} is unknown and the possibility that ATR-induced Co−C bond homolysis serves to return cob(II)alamin to the cytoplasm remains open.

Supplementary Material

Refer to Web version on PubMed Central for supplementary material.

ACKNOWLEDGMENTS

This work was supported in part by grants from the National Institutes of Health (DK45776 to R.B., 5 F32 GM113405 to G.C.C. and DK054514 to K.W.) and the National Science Foundation (CHE 1710339 to T.C.B.).

REFERENCES

(1). Hodgkin DC; Kamper J; Mackay M; Pickworth J; Trueblood KN; White JG Structure of vitamin B_{12}. Nature (London, U. K.) 1956, 178, 64–66. [PubMed: 13348621]

(2). Watkins D; Rosenblatt DS Inborn errors of cobalamin absorption and metabolism. Am. J. Med. Genet., Part C 2011, 157, 33–44.

(3). Gherasim C; Lofgren M; Banerjee R Navigating the B_{12} road: assimilation, delivery and disorders of cobalamin. J. Biol. Chem 2013, 288, 13186–13193. [PubMed: 23539619]

(4). Banerjee R Radical carbon skeleton rearrangements: catalysis by coenzyme B_{12}-dependent mutases. Chem. Rev 2003, 103 (6), 2083–2094. [PubMed: 12797824]

(5). Banerjee RV; Matthews RG Cobalamin-dependent methionine synthase. FASEB J. 1990, 4, 1450–1459. [PubMed: 2407589]

(6). Padovani D; Labunska T; Palfey BA; Ballou DP; Banerjee R Adenosyltransferase tailors and delivers coenzyme B_{12}. Nat. Chem. Biol 2008, 4 (3), 194–196. [PubMed: 18264093]

(7). Yamanishi M; Labunska T; Banerjee R Mirror ″base-off″ conformation of coenzyme B_{12} in human adenosyltransferase and its downstream target, methylmalonyl-CoA mutase. J. Am. Chem. Soc 2005, 127, 526–527. [PubMed: 15643868]

(8). Froese DS; Kochan G; Muniz JR; Wu X; Gileadi C; Ugochukwu E; Krysztofinska E; Gravel RA; Oppermann U; Yue WW Structures of the human GTPase MMAA and vitamin B_{12}- dependent methylmalonyl-CoA mutase and insight into their complex formation. J. Biol. Chem 2010, 285 (49), 38204–38213. [PubMed: 20876572]

(9). Schrauzer GN; Grate JH Sterically induced, spontaneous cobalt-carbon bond homolysis and beta-elimination reactions of primary and secondary organocobalamins. J. Am. Chem. Soc 1981, 103, 541–546.

(10). Waddington MD; Finke RG Neopentylcobalamin (Neopentyl-B_{12}) Cobalt-Carbon Bond Thermolysis Products, Kinetics, Activation Parameters, and Bond-Dissociation Energy - a Chemical-Model Exhibiting 10^6 of the 10^{12} Enzymatic Activation of Coenzyme-B_{12}s Cobalt-Carbon Bond. J. Am. Chem. Soc 1993, 115(11), 4629–4640.

(11). Stich TA; Yamanishi M; Banerjee R; Brunold TC Spectroscopic evidence for the formation of a four-coordinate Co^{2+}cobalamin species upon binding to the human ATP:cobalamin adenosyltransferase. J. Am. Chem. Soc 2005, 127 (21), 7660–7661. [PubMed: 15913339]

(12). Schwartz PA; Frey PA 5′-Peroxyadenosine and 5′-peroxyadenosylcobalamin as intermediates in the aerobic photolysis of adenosylcobalamin. Biochemistry 2007, 46 (24), 7284–7292. [PubMed: 17503776]

(13). Schubert HL; Hill CP Structure of ATP-Bound Human ATP:Cobalamin Adenosyltransferase. Biochemistry 2006, 45 (51), 15188–15196. [PubMed: 17176040]

(14). St. Maurice M; Mera P; Park K; Brunold TC; Escalante-Semerena JC; Rayment I Structural characterization of a human-type corrinoid adenosyltransferase confirms that coenzyme B_{12} is synthesized through a four-coordinate intermediate. Biochemistry 2008, 47 (21), 5755–5766. [PubMed: 18452306]

(15). Kim J; Gherasim C; Banerjee R Decyanation of vitamin B_{12} by a trafficking chaperone. Proc. Natl. Acad. Sci. U. S. A 2008, 105(38), 14551–14554. [PubMed: 18779575]

(16). Kim J; Hannibal L; Gherasim C; Jacobsen DW; Banerjee R A human vitamin B_{12} trafficking protein uses glutathione transferase activity for processing alkylcobalamins. J. Biol. Chem 2009, 284 (48), 33418–33424. [PubMed: 19801555]

(17). Hannibal L; Kim J; Brasch NE; Wang S; Rosenblatt DS; Banerjee R; Jacobsen DW Processing of alkylcobalamins in mammalian cells: A role for the MMACHC (cblC) gene product. Mol. Genet. Metab 2009, 97 (4), 260–266. [PubMed: 19447654]

(18). Lerner-Ellis JP; Gradinger AB; Watkins D; Tirone JC; Villeneuve A; Dobson CM; Montpetit A; Lepage P; Gravel RA; Rosenblatt DS Mutation and biochemical analysis of patients belonging to the cblB complementation class of vitamin B12-dependent methylmalonic aciduria. Mol. Genet. Metab 2006, 87 (3), 219–225. [PubMed: 16410054]

(19). Park K; Mera PE; Escalante-Semerena JC; Brunold TC Spectroscopic characterization of active-site variants of the PduO-type ATP:corrinoid adenosyltransferase from Lactobacillus reuteri:

insights into the mechanism of four-coordinate Co(II)corrinoid formation. Inorg. Chem 2012, 51 (8), 4482–4494. [PubMed: 22480351]

(20). Lexa D; Saveant JM Electrochemistry of vitamin B_{12}. I. Role of the base-on/base-off reaction in the oxidoreduction mechanism of the B_{12r}-B_{12s} system. J. Am. Chem. Soc 1976, 98, 2652–2658. [PubMed: 4489]

(21). Shen H; Campanello GC; Flicker D; Grabarek Z; Hu J; Luo C; Banerjee R; Mootha VK The Human Knockout Gene CLYBL Connects Itaconate to Vitamin B_{12}. Cell 2017, 171 (4), 771–782. [PubMed: 29056341]

(22). Oltean S; Banerjee R A B_{12}-responsive IRES element in human methionine synthase. J. Biol. Chem 2005, 280 (38), 32662–8. [PubMed: 16051610]

(23). Chen Z; Chakraborty S; Banerjee R Demonstration that the mammalian methionine synthases are predominantly cobalamin-loaded. J. Biol. Chem 1995, 270, 19246–19249. [PubMed: 7642596]

(24). Kennedy DG; Cannavan A; Molloy A; O'Harte F; Taylor SM; Kennedy S; Blanchflower WJ Methylmalonyl-CoA mutase (EC 5.4.99.2) and methionine synthetase (EC 2.1.1.13) in the tissues of cobalt-vitamin B_{12} deficient sheep. Br. J. Nutr 1990, 64 (3), 721–732. [PubMed: 1979918]

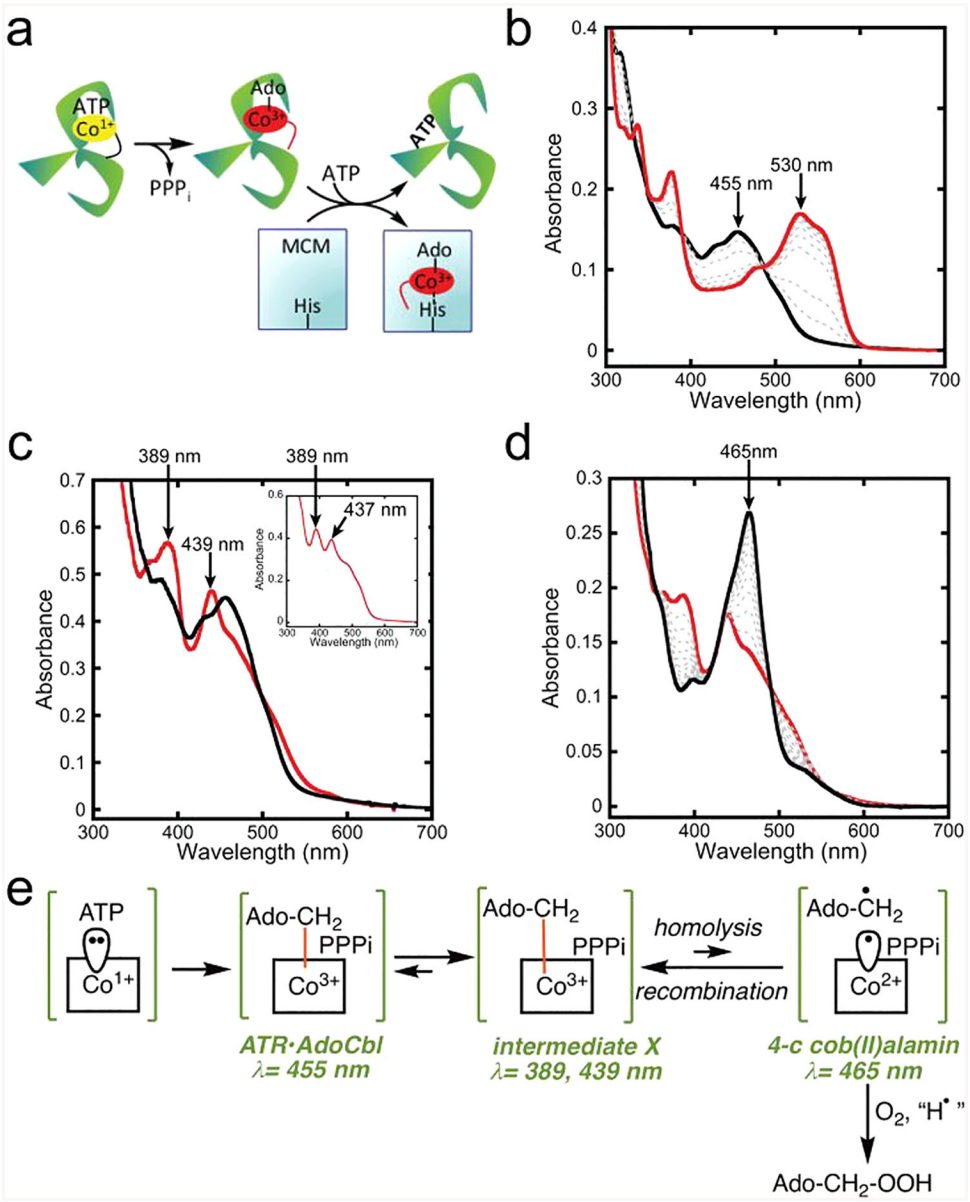

Figure 1.

PPP_i induces Co−C homolysis in ATR-bound AdoCbl. (a) Scheme showing the role of ATR (green) in AdoCbl synthesis and transfer to MCM. (b) Transfer of AdoCbl from ATR (black) to MCM (red). (c) Addition of PPP_i to AdoCbl bound to ATR (black) results in the formation of intermediate X (red) under anaerobic conditions. Inset shows the spectrum of base-off NpCbl. (d) Under aerobic conditions, X (red) converts to 4C cob(II)alamin (black). (e) Scheme showing conversion of ATR-bound AdoCbl to X and to 4C cob(II)alamin and 5′-hydroperoxyadenosine.

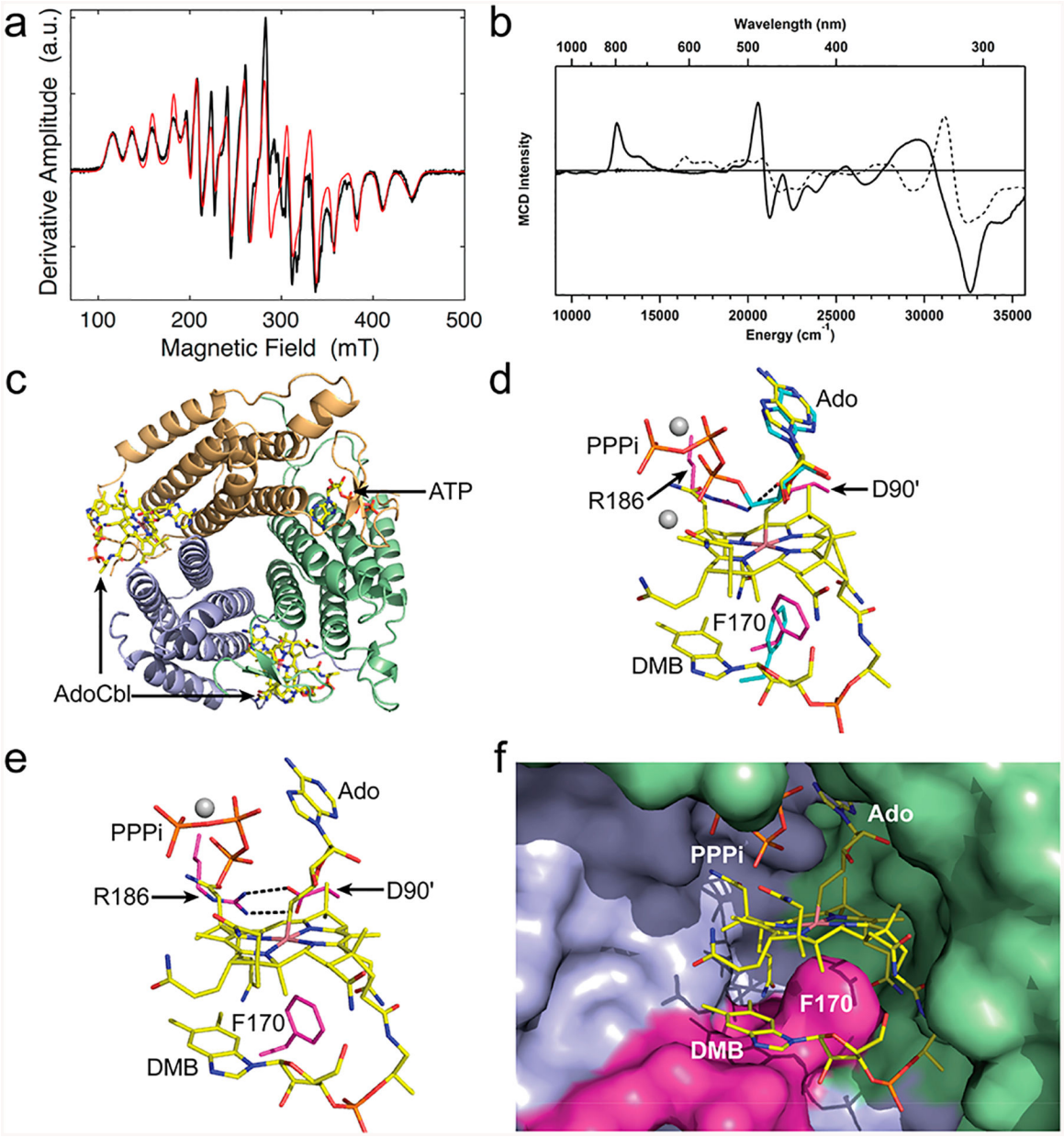

Figure 2.

Spectroscopic and structural characterization of B_{12} bound to ATR. (a) EPR spectrum of 4C cob(II)alamin formed after addition of PPP_i under aerobic conditions (black). The red line corresponds to the simulated spectrum. (b) MCD spectra of 4C cob(II)alamin (solid line) generated under the same conditions as (a) and of 5C cob(II)inamide (dashed lines) as a reference. (c) Structure of human ATR showing two subunits occupied by AdoCbl and a third by ATP.(d) Superposition of the adenosine rings in ATP (cyan, PDB: 21DX) and AdoCbl (yellow, PDB: 6D5K, this study) bound to ATR. (e) Close-up of the ATR·AdoCbl·PPP_i active site structure (PDB: 6D5X, this study). (f) Close-up of human ATR showing that the DMB tail, tucked below the corrin ring, is kept from coordinating to the

cobalt by Phe170 on a hydrophobic loop (pink). Adjacent subunits that form the active site are in blue and green. The gray spheres in panels d and e represent magnesium.

a

Group	%AdoCbl	n	p-value
Control	15.1 ± 3.4	192	-
mut (total)	8.1 ± 5.0	248	<0.0005
mut^0	8.1 ± 4.4	195	<0.0005
mut$^-$	8.3 ± 6.9	53	<0.0005
cblB	3.0 ± 2.1	45	<0.0005

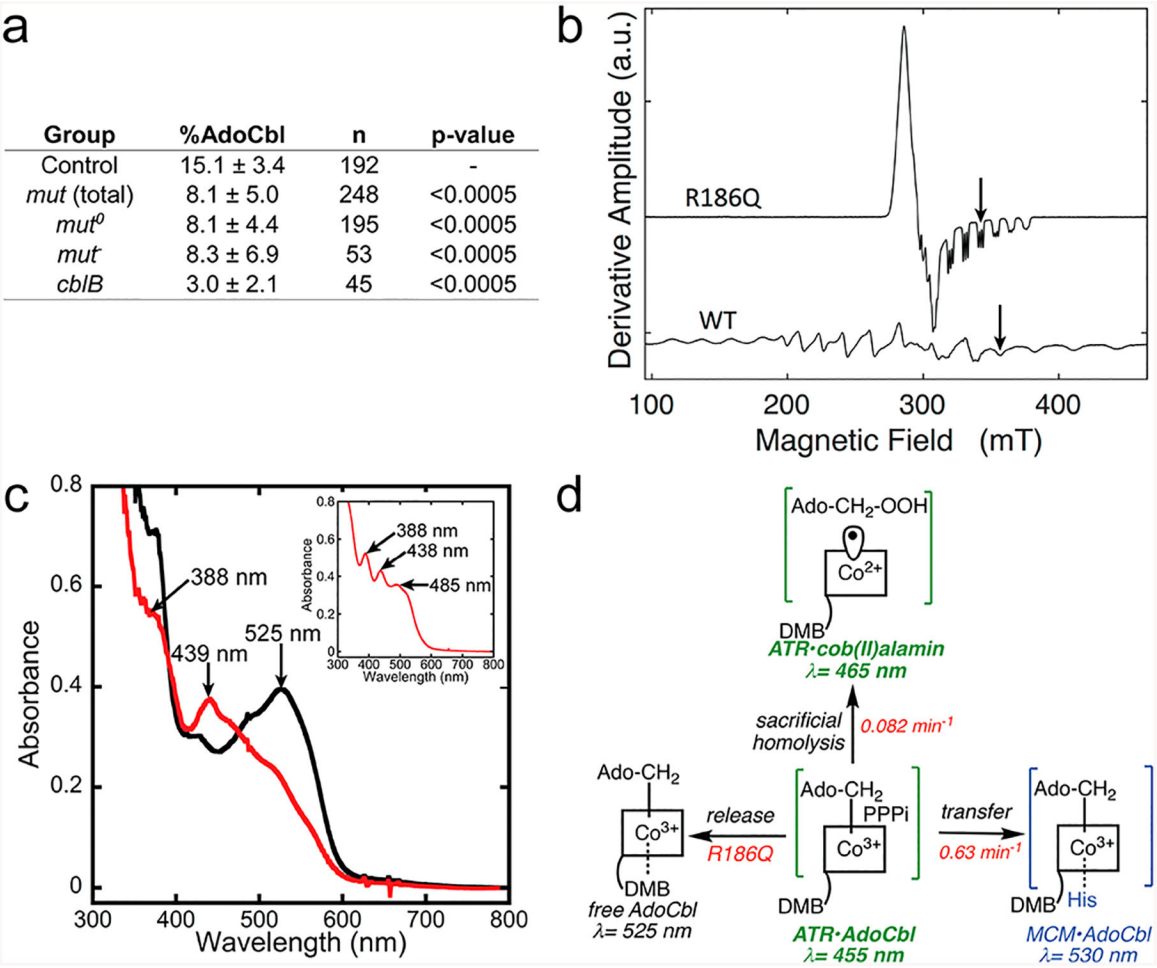

Figure 3.

Impact of ATR deficiency on AdoCbl synthesis. (a) AdoCbl as a percent of total cobalamin in fibroblasts from ATR (*cblB*) or MCM (*mut*) deficiency versus control individuals. The *mut*$^-$ and *mut*^{0} subgroups represent fibroblasts with diminished or undetectable MCM activity, respectively. (b) Comparison of the EPR spectra of cob(II)alamin bound to R186Q versus wild-type (WT) ATR. The presence of the triplet superhyperfine splittings in the high-field lines of the R186Q spectrum is caused by the presence of axial nitrogen coordination (absent in WT). (c) Absorbance spectrum of 6C AdoCbl bound to R186Q ATR (black). Addition of PPP_i under anaerobic conditions gives rise to a spectrum (red) that resembles “base-on” NpCbl (inset). (d) Intermediate X partitions between transfer to MCM, release into solution or undergoes sacrificial Co−C bond homolysis leading to retention of tightly bound cob(II)alamin.